

UNIVERSITY OF MINNESOTA
ST. ANTHONY FALLS HYDRAULIC LABORATORY
LORENZ G. STRAUB, Director

Technical Paper No. 23, Series B

The Sonic Surface-Wave Transducer

Preprint of Paper to be Presented at the
American Towing Tank Conference, University of California, Berkeley Campus,
August 31 to September 2, 1959

by
JOHN M. KILLEN



July 1959
Minneapolis, Minnesota

UNIVERSITY OF MINNESOTA
ST. ANTHONY FALLS HYDRAULIC LABORATORY
LORENZ G. STRAUB, Director

Technical Paper No. 23, Series B

The Sonic Surface-Wave Transducer

Preprint of Paper to be Presented at the
American Towing Tank Conference, University of California, Berkeley Campus,
August 31 to September 2, 1959

by
JOHN M. KILLEN



July 1959
Minneapolis, Minnesota

A B S T R A C T

A wave height measuring instrument is described which measures the height of water surface waves by means of a sonic ranging technique in air. This system is advantageous for wave amplitude measurements from a moving towing carriage since the sensing elements or its supports do not disturb the water surface.

The design operating range of the instrument is 2-in. to 2-ft wave height. The accuracy of measurement depends on the incremental slope of the water surface at the point of measurement. An intrinsic error of ± 0.8 per cent average over the wave would occur for a 2-ft wave with a slope at mid-height of 0.2. This error increases to ± 3.2 per cent for a 2-in. wave of the same slope. The error is much reduced for both these conditions with less steep waves.

C O N T E N T S

	Page
Abstract	iii
List of Illustrations	v
I. INTRODUCTION	1
II. DESCRIPTION OF APPARATUS	1
III. ACCURACY OF MEASUREMENT	2
IV. CIRCUIT DESCRIPTION	5
A. Pulser	5
B. Spark Coil and Gap	5
C. Microphone	6
D. Amplifier and Amplitude Discriminator	6
E. Phantastron Delay	6
F. Bootstrap Sweep	6
G. Holding Circuits	6
V. ACKNOWLEDGMENTS	7
List of References	8
Figures 1 through 15	11
Parts List	27

L I S T O F I L L U S T R A T I O N S

Figure		Page
1	Photograph of Front Panel	11
2	Photograph of Ranging Head	12
3	Large Mechanical Wave H = 2 ft, $\lambda = 40$ ft	13
4	Small Mechanical Wave H = 2 in., $\lambda = 2$ ft	14
5	Photographs of Towing Carriage and Mechanical Waves	15
6	Comparison of Capacitive Wave Record with Sonic Wave Record, H = 0.693 ft, Steepness = 0.055	16
7	Comparison of Capacitive Wave Record with Sonic Wave Record, H = 1 ft, Steepness = 0.125	17
8	Functional Block Diagram of Sonic Wave-Profile Transducer . .	18
9	Microphone and Preamplifier Housing	19
10	Frequency Response of Preamplifier	20
11	Pulser	21
12	Delay Phantastron and Amplitude Discriminator	22
13	Amplifiers	23
14	Bootstrap Sweep and Holding Circuits	24
15	Power Supplies	25

T H E S O N I C S U R F A C E - W A V E T R A N S D U C E R

I. INTRODUCTION

The use of a wave-profile recorder whose sensing elements are submerged or partly submerged and which is mounted on a towing carriage moving at high speed produces problems of structural support of the element and disturbance of the liquid surface. The wave-profile recorder described in this report is based on the sonic-ranging principle in air and appears to overcome these difficulties since no part of the instrument contacts the water surface.

The instrument is intended to operate with wave heights of 2 in. to 2 ft, wave lengths of 2 to 40 ft, and an "equivalent period" as short as 1/20 sec. These operating ranges are presumed to correspond to ranges of interest in laboratory wave studies and do not specify the limits of application. The obtainable accuracy is dependent on the incremental slope and the wave height. Therefore, with this instrument, as with most physical measuring instruments, careful attention must be paid to these two mentioned geometries in order to keep errors within the acceptable limits for the particular investigation.

II. DESCRIPTION OF APPARATUS

The instrument functions as follows: A very short pulse of sound is transmitted from a point as close as practical to the water surface. The sound pulse is reflected by the water surface and sensed by a microphone located as close as possible to the point of transmission. Appropriate electronic circuits measure the time of travel of the sound pulse and convert this time into a voltage proportional to the time. When this process is repeated 120 times a second, a voltage output results whose magnitude varies with the changes in the level of the water surface. On a cathode-ray oscillograph or light-beam oscillograph which have a high-frequency response, this wave profile will appear composed of a series of small steps, each step corresponding to a sample of the wave profile. On most direct-writing oscillographs whose frequency response extends to about 100 cycles, the wave profile will appear as a smooth line.

The instrument is composed of two parts: a control panel, Fig. 1, and a ranging head, Fig. 2. In practical application the ranging head is placed approximately 5.5 in. from the maximum expected crest of the waves. The ranging head can be attached to some positioning device for ease of operation and calibration.

A "stepped" range control on the control section panel permits like adjustment of the system sensitivity for a wave height of 2 in. to 2 ft.

III. ACCURACY OF MEASUREMENT

The pulse of sound emitted by the transmitter behaves as a spherical wave. As a result the apparatus measures the shortest distance from the transmitter to the water surface and return. On sloping surfaces this shortest distance is to a point slightly displaced from directly below the transmitter. This would not cause error if the point of reflection were known. It is usually necessary to assume the reflection point is directly below the transmitter; this produces a small error in the above measurement.

If the transmitting spark and the microphone diaphragm are considered to be the foci of an ellipse which is tangent to the water surface at the point of reflection, the following expression for error can be developed from the optical properties of the ellipse.

$$\% \text{ error} = \frac{100r}{H} \left[\left(\frac{1}{\cos^2 \theta} - \frac{c^2}{4r^2} \right)^{1/2} - 1 \right] \quad (1)$$

where r = measured distance (wave amplitude plus 5-1/2 in.)
 H = wave length *height*
 c = separation of spark and microphone
 θ = angle of a tangent to the water surface at the point of reflection with the horizontal

This expression shows an upward shift of the recorded crest and trough which is not the same at the respective points, resulting in an error in wave height measurement. If the separation of the spark and transmitter is made sufficiently small, this error can be neglected and the expression for per cent error becomes

$$\% \text{ error} \approx \frac{50rs^2}{H} \quad (2)$$

S = the incremental slope of the water surface at the measuring point

As an example, consider the two extremes of waves with (1) a height of 2 in. and a length of 2 ft, and (2) a height of 2 ft and a length of 40 ft. For the 2-in. wave, Eq. (1) shows an error in measured height of 1/2% and an error in amplitude on the slope at mid-point of 7.0%.

The error on the 2-ft wave is 0.94% on the mid-slope and negligible on the crest. When the instrument has a relative motion with respect to the wave whose profile it is measuring, two additional sources of error arise. Both these, however, produce a phase shift of the entire wave pattern in the direction of motion and therefore should not cause any great difficulty.

First there will be a small displacement of the record due to the finite velocity of propagation of the sound. With a maximum sound path of 5 ft for the 2-ft wave and a carriage speed of 20 fps, there will be a shift of 0.1 ft. For $\lambda = 2.0$, and $H = 2$ in., there would be a phase shift of 1.8 degrees at the troughs and 0.016 ft or 0.3 degrees at the crests.

The second cause of phase shift is due to sampling and filtering. The filtering action of the recorder system on the "stepped" output of the sonic wave transducer results in a time delay which can be as great as one-half the sampling period [1].* Under the assumption of a constant delay, the wave profiles at various velocities were delayed in proportion to a constant multiplied by velocity at each point.

The combined effect of all the errors mentioned is shown in Figs. 3 and 4. These are experimental points on two waves constructed of sheet metal with a trochoidal shape with dimensions indicated on the figures. The sheet-metal waves, while only approximating a water wave, have the advantage of possessing an easily measurable slope and height at any point and consequently

*Numbers in brackets refer to the corresponding numbers in the List of References on p. 8.

are useful for evaluating the behavior of the measuring device. The profile measured by a point gage is shown as a solid line with data points as circles, and a profile taken at very low speed with the sonic transducer with data points as triangles is shown as a second line. The voltage output in this case was measured by a potentiometer because the oscillograph pen was not sufficiently accurate to show the resolution capabilities of the instrument. The error arising from the motion of the towing carriage has been corrected on the basis of estimated phase shifts in the recorder. As mentioned in the preceding paragraph, it will be noted that this correction brings the dynamic recording into close conformity with the static record. Only a few points are shown since it was difficult to establish the instantaneous position of the moving towing carriage. At the point shown, cams on the tracks activated the marker points. The sonic record and the point-gage difference which arises from geometric error can be resolved by application of Eq. (2).

Figures 6 and 7 show a comparison of the same two water waves as recorded by a capacitive wave recorder and the sonic-wave recorder system. The steepness shown in Fig. 7 is in excess of the steepness recommended for recording with the sonic transducer. When this instrument is used in the presence of objects other than the water surface (such as boat models, towing-carriage support members, channel walls, etc.), the distance from the ranging head to the nearest point on the object must be greater than the maximum distance from the ranging head to the trough of a wave. A flat surface above the ranging head, a distance less than the maximum distance from the ranging head to the water surface, should also be avoided. Both of these conditions can result in the instrument's ranging on the solid object instead of on the wave surface, whenever the wave is a greater distance from the ranging head than the solid object is from the ranging head. When the presence of interfering objects cannot be avoided, a layer of glass wool over the offending surface can usually reduce its effect to a negligible value.

In operations involving more than one unit, interference from the direct transmission of the second unit would result unless the direct-transmission path were greater than the total path of the sound from the ranging head to the trough and return under the condition that all units were designed to "trigger" the spark simultaneously.

IV. CIRCUIT DESCRIPTION

An overall block diagram (Fig. 8) shows the sequence of functions performed by the individual elements described below.

A. Pulser

The Thyatron V_3 (Figs. 8 and 11) provides a pulse of current for the transmitter by discharging a condenser through the winding of the primary of the spark coil. The thyatron is triggered at 120 cycles per sec by the power line.

B. Spark Coil and Gap

The discharge of the spark coil energy through a short gap produces the sound energy for echo ranging.

This sound energy has the nature of a weak shock whose speed of propagation is very nearly that of sound in air and has a steep leading edge which is quite suitable for this application.

The first half cycle corresponds roughly to a 100-kc sine wave with a peak pressure on the order of 300 to 500 dynes per sq cm at a distance of 60 cm. This amplitude varies considerably with various gap widths. The gap width can be used to adjust the intensity of the transmitted pulse when required.

Some small error in measurement is introduced by the "build-up time" of the voltage across the gap before gap breakdown. The breakdown does not occur at the same time with successive discharges, but this variation is sufficiently small to be ignored.

It has been found that smooth operation of the spark depends on the surface of the electrodes. Sanding of the electrode with a fine emery cloth will restore smooth performance when the spark has become erratic. This appears necessary approximately after every 4 hrs of operation. The duration of operation between cleanings has been found to vary with different materials. Electrode material from oil burner ignition electrodes has been found most satisfactory to date.

C. Microphone

The receiver is a solid dielectric condenser microphone described in Reference [2]. Its construction details are shown in Fig. 9. The film used as a diaphragm is plated mylar of approximately 0.0005 in. thickness.

The microphone frequency response is nearly uniform to 1 megacycle. The transistor preamplifier has a frequency response as shown in Fig. 10. The low sensitivity in the frequency range below 20 kc reduces the interference from ambient noise to a very low value because of the high attenuation of the high frequencies in air.

D. Amplifier and Amplitude Discriminator

The pulse discriminator is a one-shot cathode-coupled multivibrator whose purpose is to discriminate against noise by acting only when the signal level rises above a certain value. It also provides a sharp pulse to terminate the timing process as precisely as possible. Amplifier $V_{37,38}$ (Fig. 13) is a plug-in unit. Its purpose is to provide sufficient voltage to operate the discriminator.

E. Phantastron Delay

This circuit provides a 300- μ second delay to permit equilibrium to be re-established after the circuit is disturbed by the transmitting pulse and to increase the resolution of the succeeding timing circuitry.

Since the accuracy of measurement depends on the accuracy of the entire timing unit, this delay must be very stable. The phantastron appears satisfactory in this application. This unit is manufactured by the Engineering Electronic Corporation of Pasadena.

F. Bootstrap Sweep

The bootstrap sweep circuit, Reference [4], is a negative feedback-type sweep generator that develops a series of voltage pulses of triangular shape whose amplitudes are proportional to the time from "switch off" of the phantastron delay until the amplitude discriminator is returned to "rest condition" by the echo. Time duration measurements are converted in this way to voltage amplitude measurements.

G. Holding Circuits

The output of the bootstrap sweep is a series of triangular pulses of varying amplitude and duration which would not be very suitable for use by a direct-writing oscillograph. The holding circuits provide a preliminary filtering. The first circuit charges a condenser C_{23} to the peak of the bootstrap output. This charge is held until the start of the next pulse when it is discharged by V_{22} to the value of the bootstrap voltage at that instant. This results in a series of voltage steps which correspond to wave heights and a superimposed negative triangular voltage. The second holding circuit charges a condenser C_{49} to the value of the condenser voltage C_{23} of the first holding circuit during its "hold period." The resultant output voltage is a series of steps which approximate the form of the water wave. The low pass filter action of the succeeding recorders smooth this output into a continuous line. This whole process of sampling and detection could be interpreted analogously to techniques of sampling and detection in a pulse-time modulation system.

V. ACKNOWLEDGMENTS

This instrument was developed and constructed by the St. Anthony Falls Hydraulic Laboratory for the David Taylor Model Basin under contract Nobs 72117, Task Order III.

The developmental program was under the general direction of Dr. Lorenz G. Straub, Director of the St. Anthony Falls Hydraulic Laboratory. The developmental program was supervised by John M. Killen; Frank Schiebe, Goffe Erickson, and Norman Viss did the experimental testing, developing, and constructing. In addition, their numerous suggestions and clarifications deserve special acknowledgment.

The editorial preparation was under the general direction of Loyal Johnson, the manuscript was prepared by Delores Grupp, and the drawings were prepared by Frank Tsai.

L I S T O F R E F E R E N C E S

- [1] Black, H. S. Modulation Theory. New York: D. Van Nostrand, 1953.
- [2] Kuhl, W. "Condenser Transmitters and Microphones." Acustica, Vol. 4, pp. 513-539. 1954.
- [3] National Bureau of Standards. Handbook Preferred Circuits. Washington, D. C.: Superintendent of Documents, U. S. Government Printing Office, 1955.
- [4] MIT Radar School Staff. Principles of Radar. New York: McGraw-Hill, 1944.

F I G U R E S
(1 through 15)

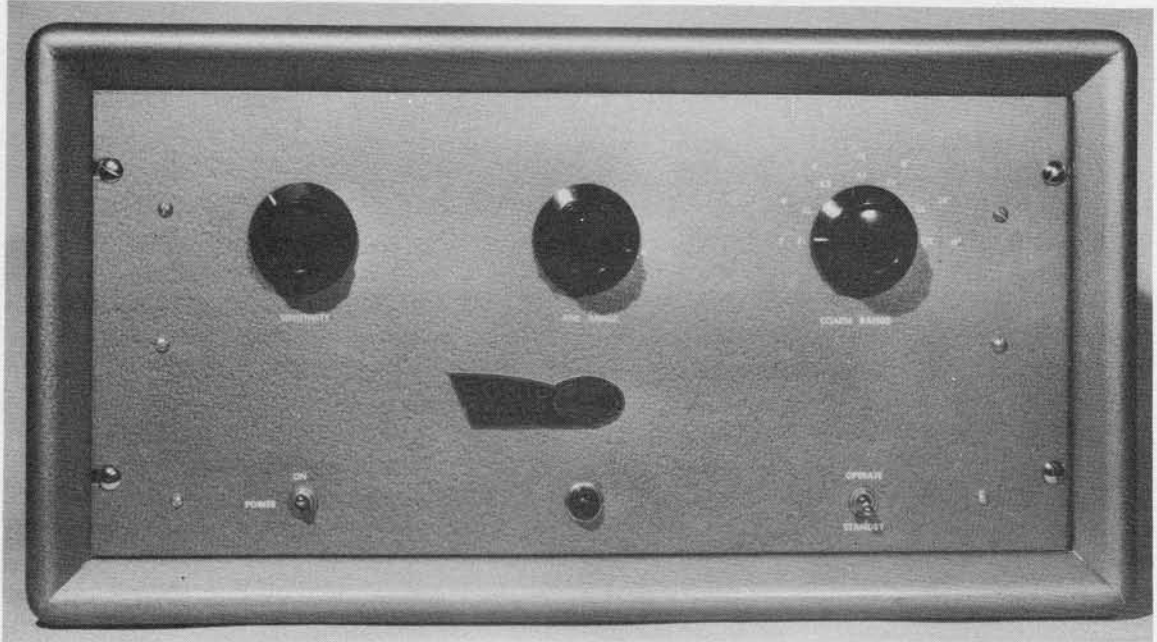


Fig. 1 - Photograph of Front Panel

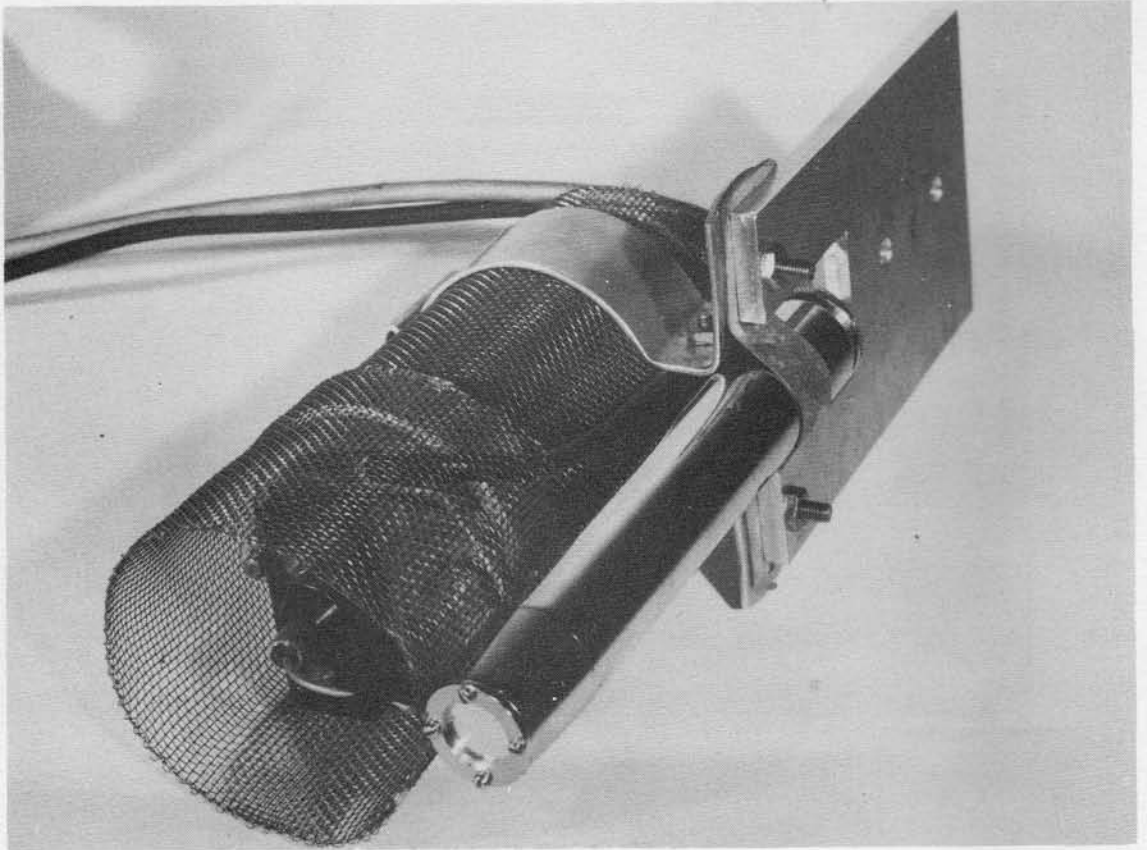


Fig. 2 - Photograph of Ranging Head

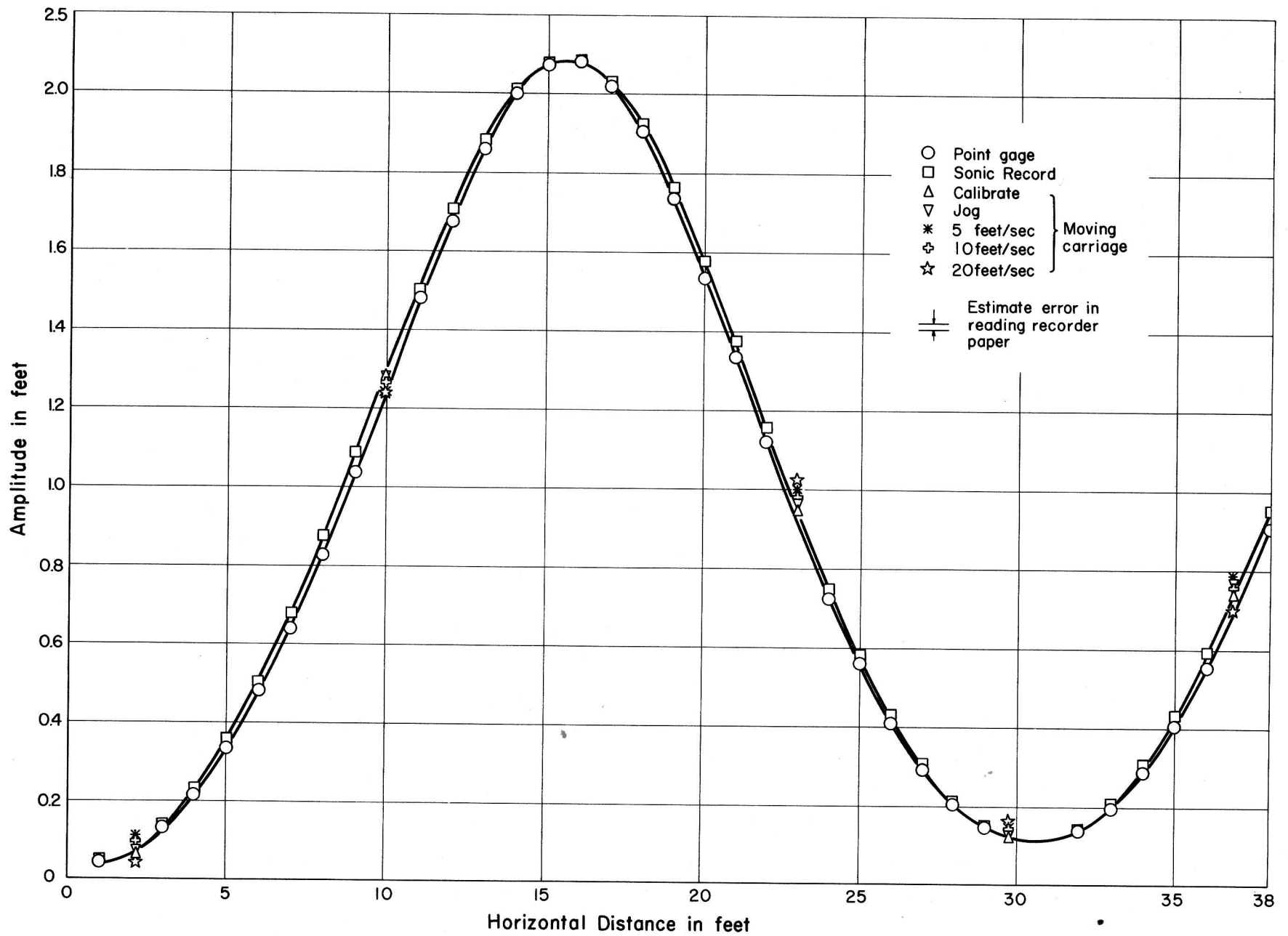


Fig. 3 - Large Mechanical Wave $H = 2$ ft, $\lambda = 40$ ft

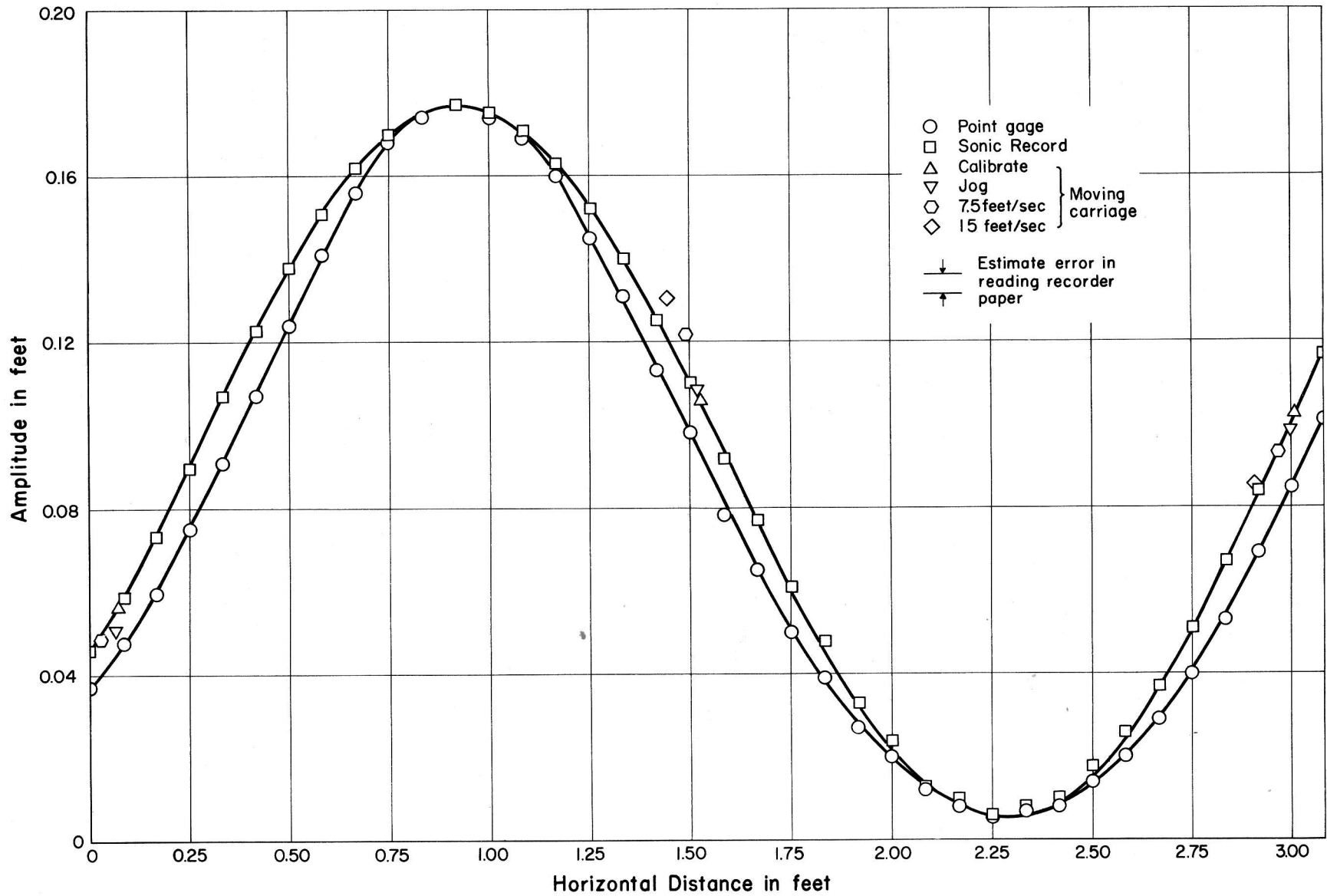


Fig. 4 - Small Mechanical Wave $H = 2$ in., $\lambda = 2$ ft

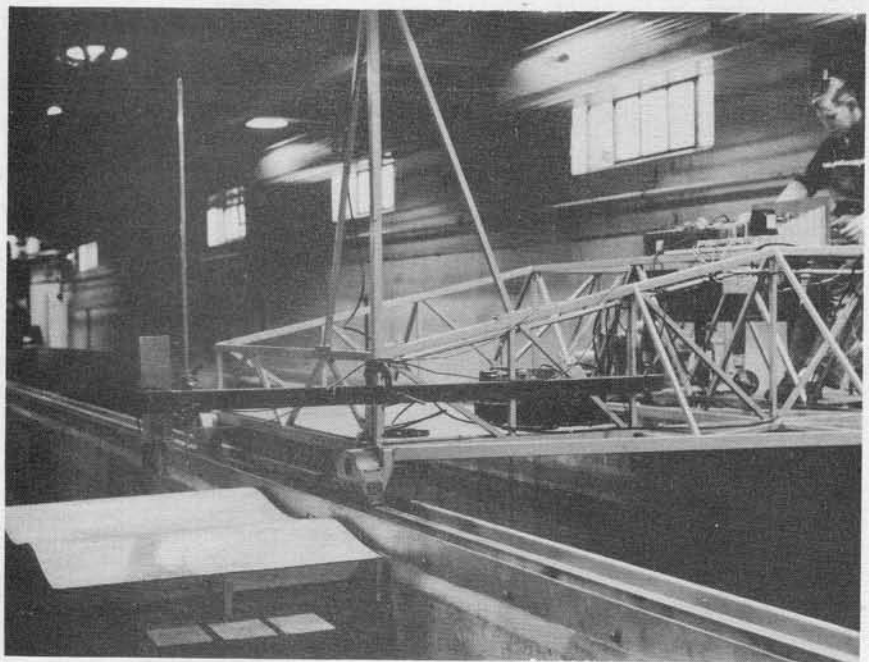
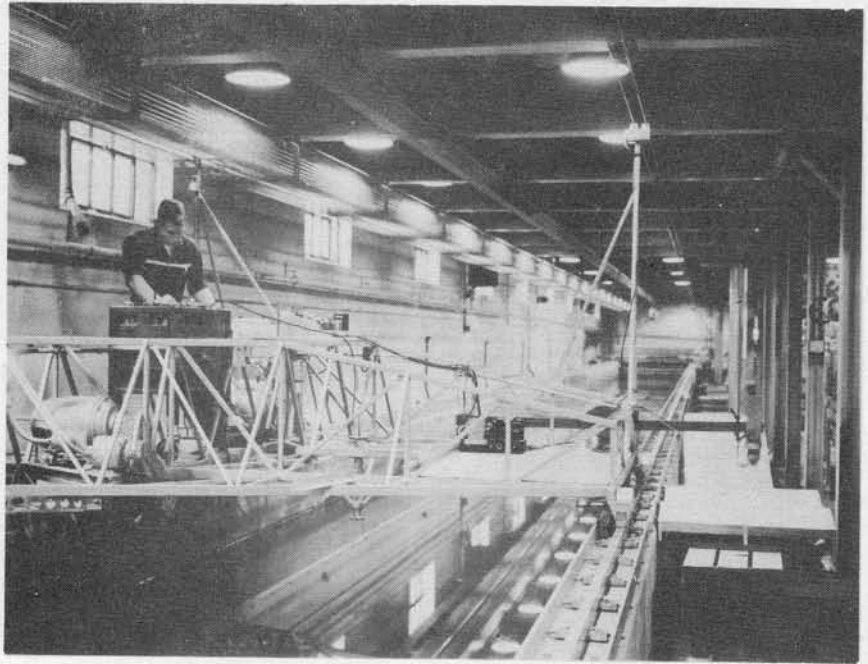
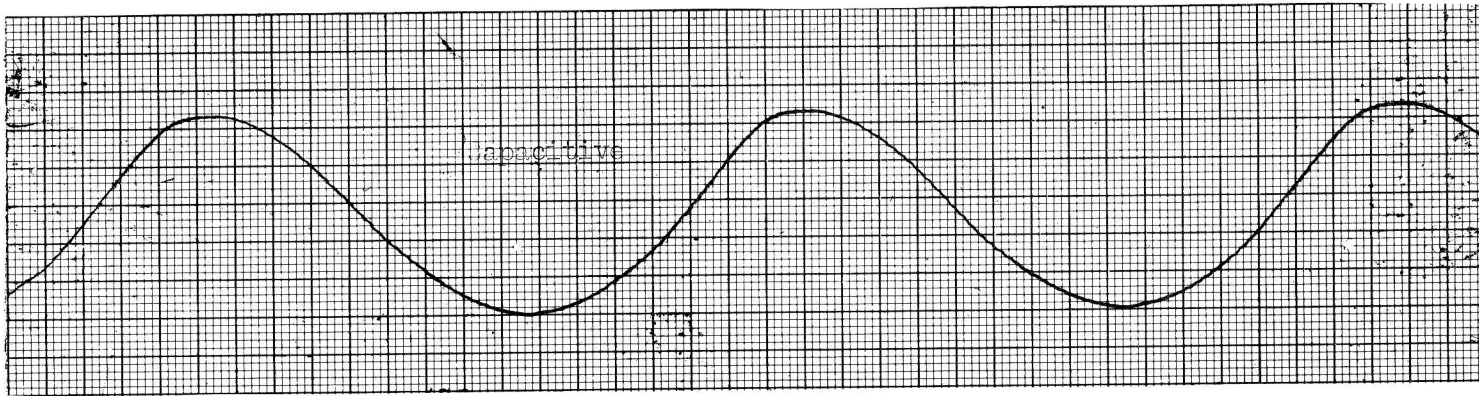
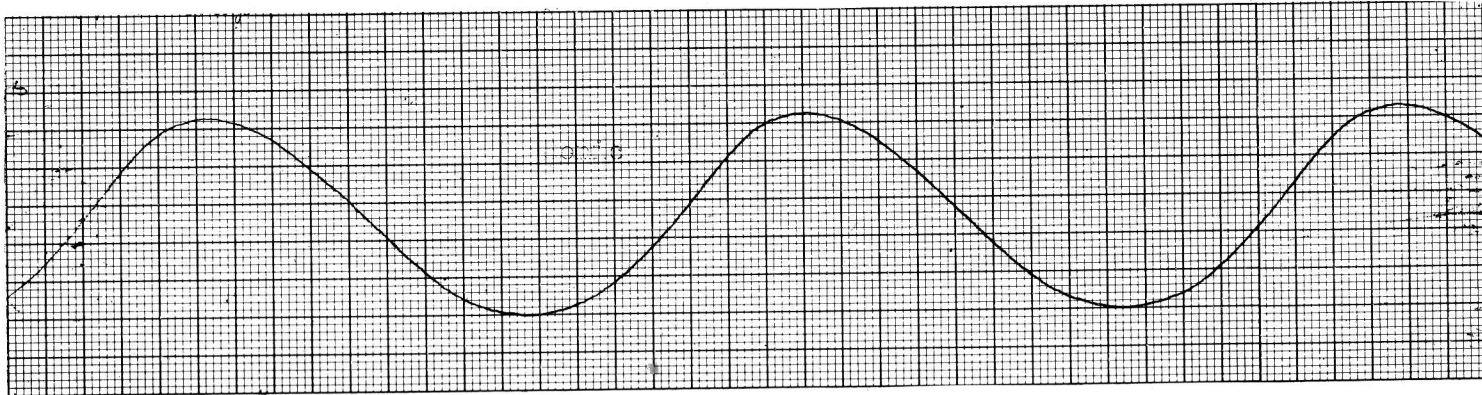


Fig. 5 - Photographs of Towing Carriage
and Mechanical Waves

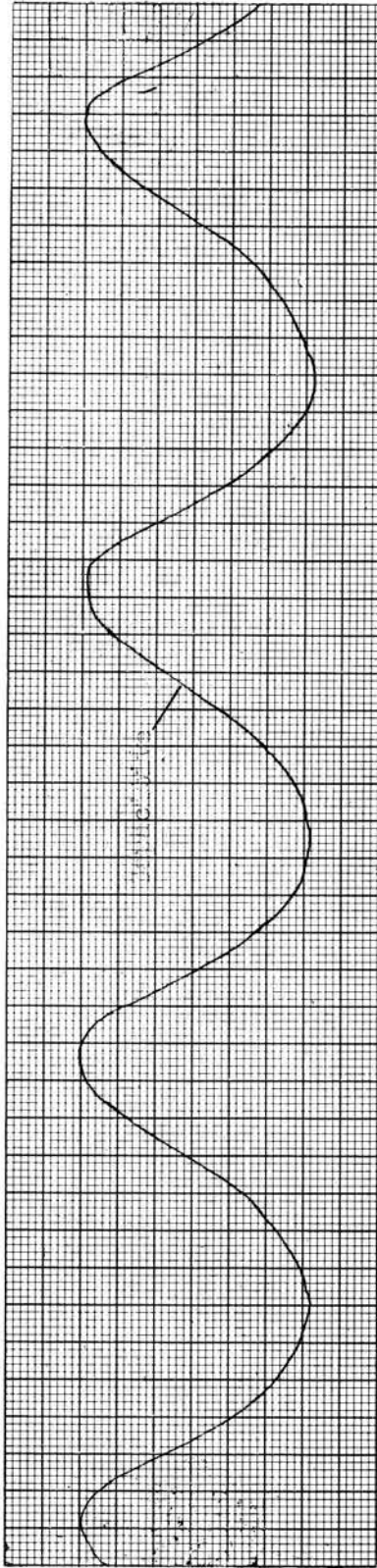


Capacitive

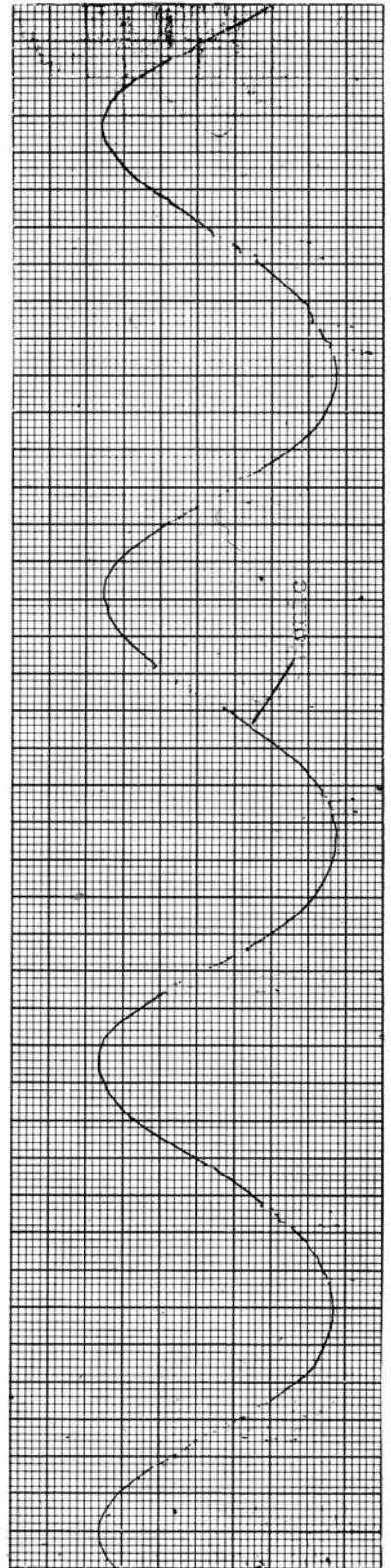


Sonic

Fig. 6 - Comparison of Capacitive Wave Record with Sonic Wave Record,
 $H = 0.693$ ft, Steepness = 0.055



Capacitive



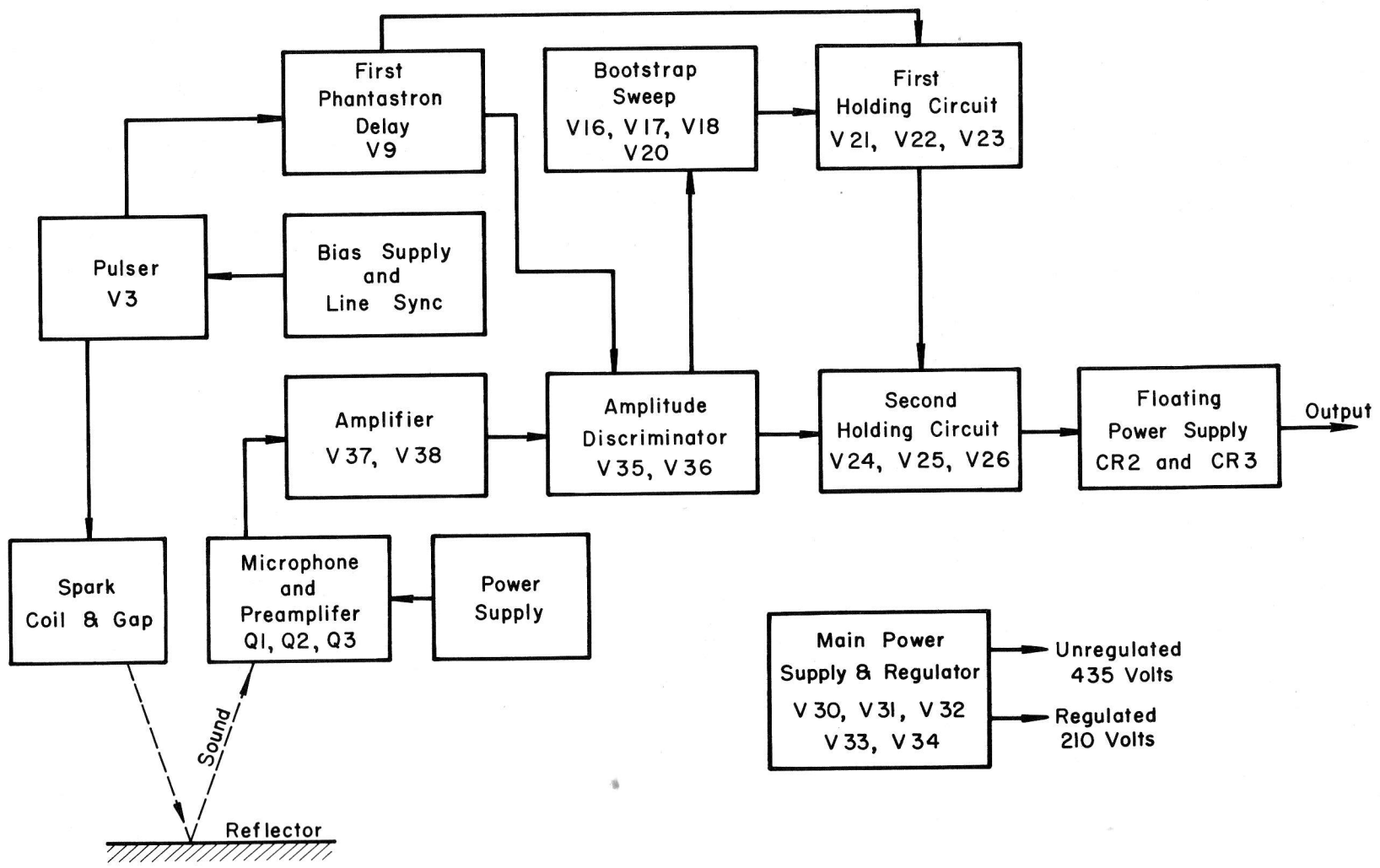


Fig. 8 - Functional Block Diagram of Sonic Wave-Profile Transducer

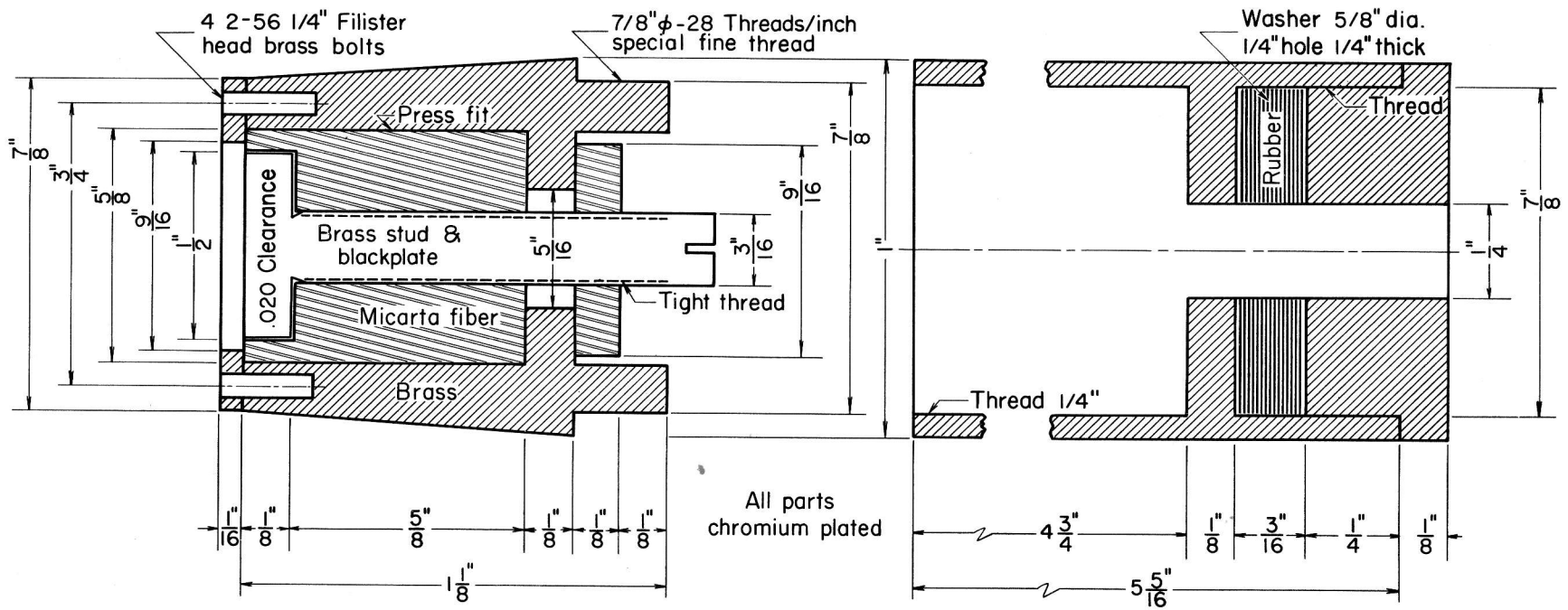


Fig. 9 - Microphone and Preamplifier Housing

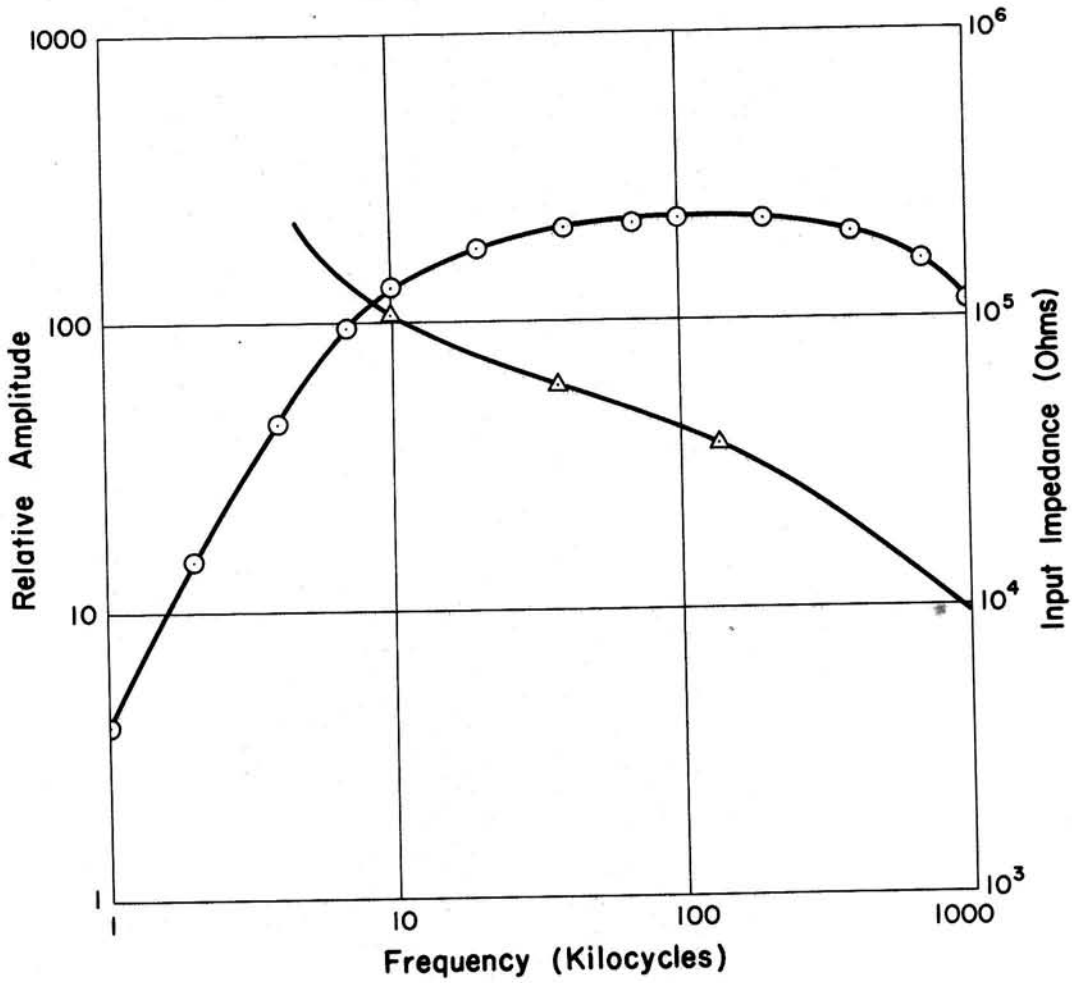


Fig. 10 - Frequency Response of Preamplifier

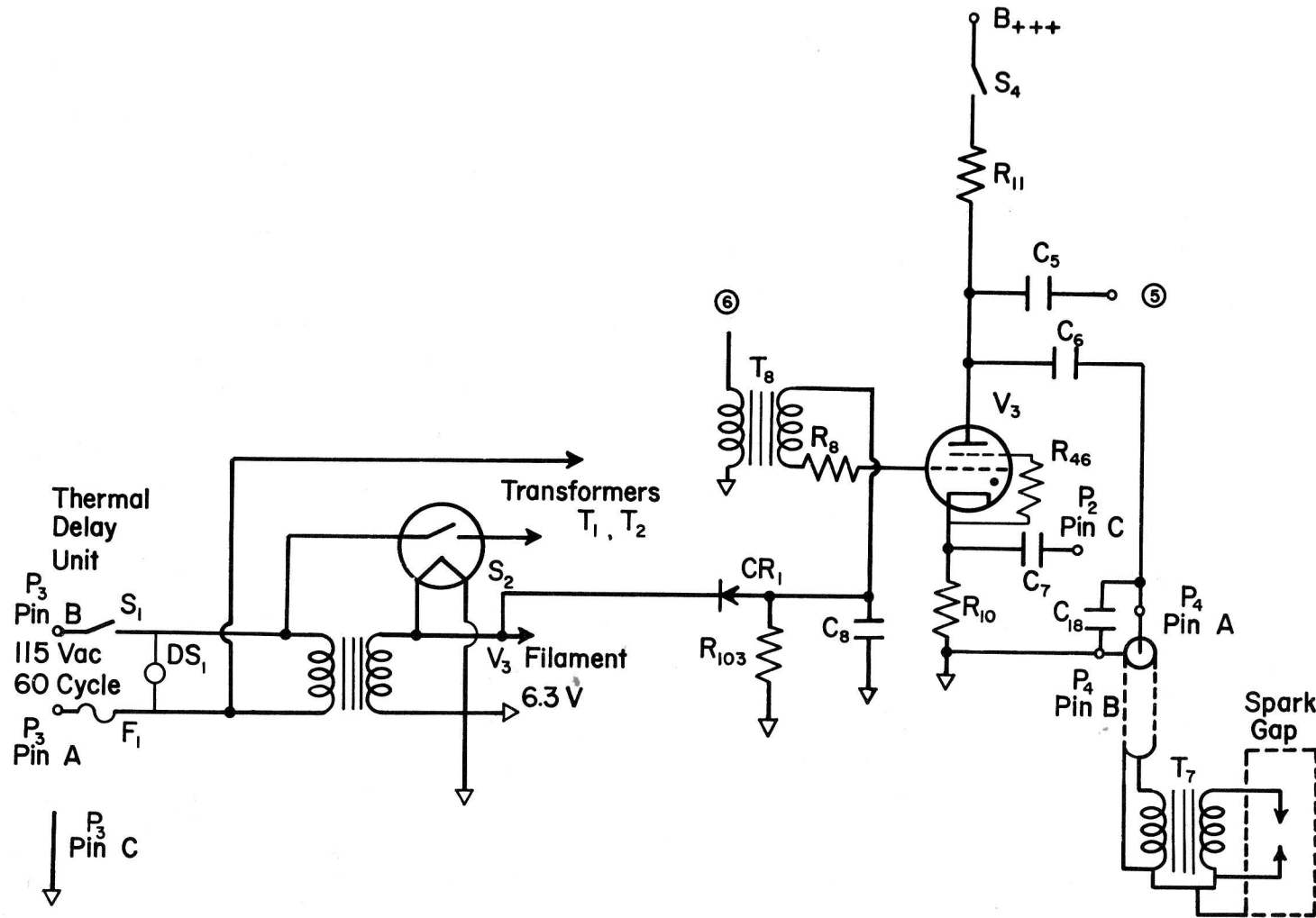


Fig. 11 - Pulser

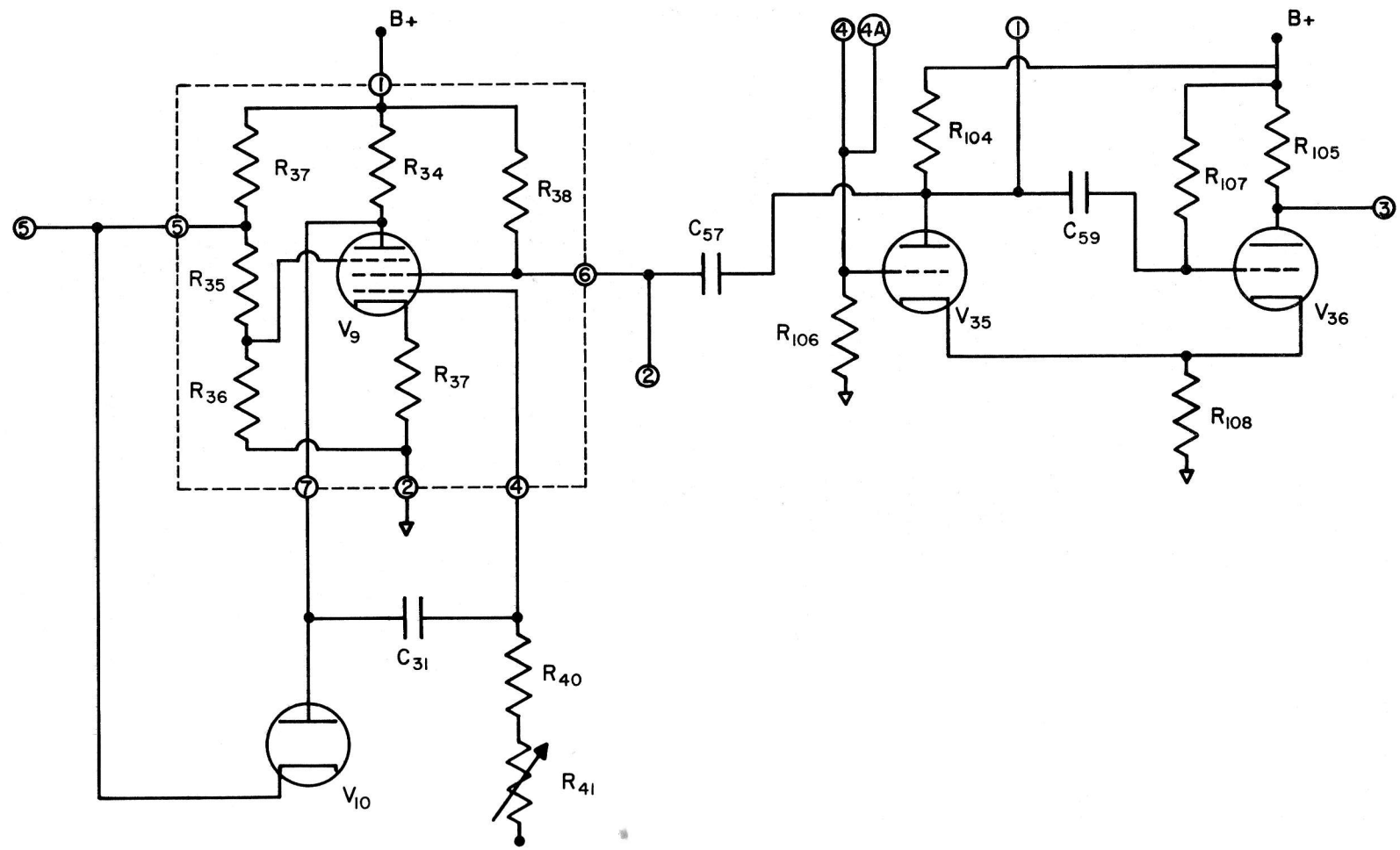


Fig. 12 - Delay Phantastron and Amplitude Discriminator

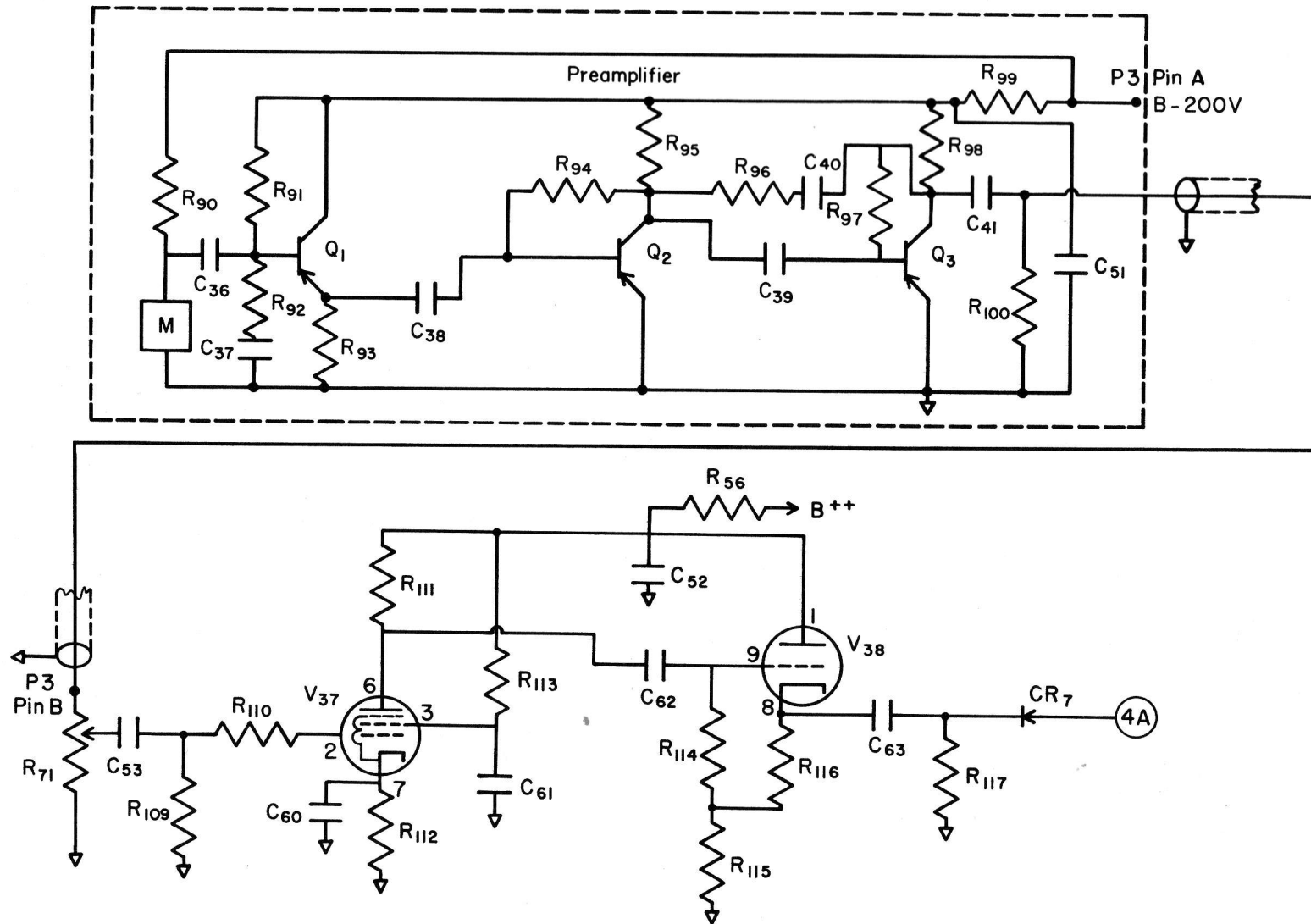


Fig. 13 - Amplifiers

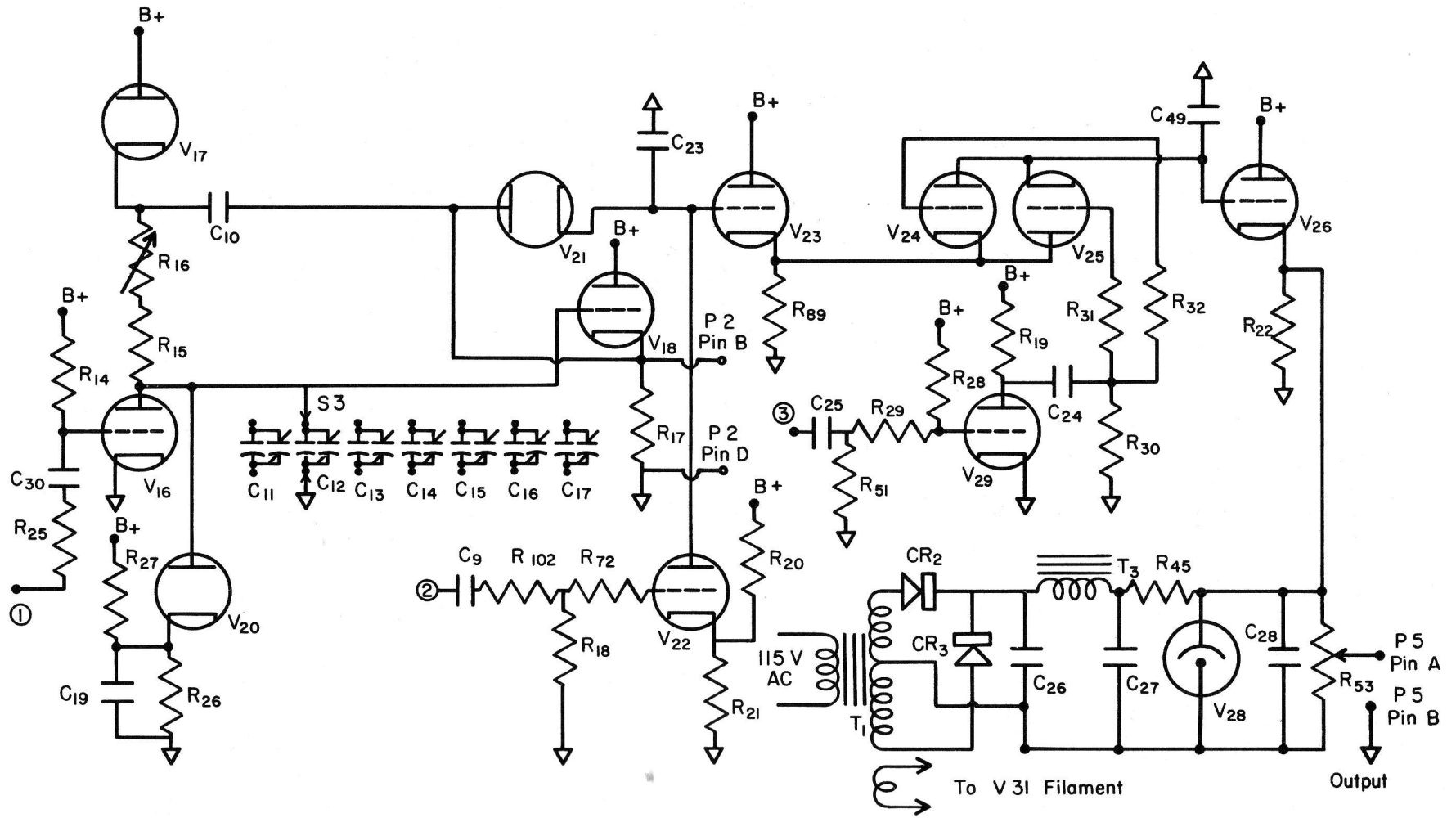


Fig. 14 - Bootstrap Sweep and Holding Circuits

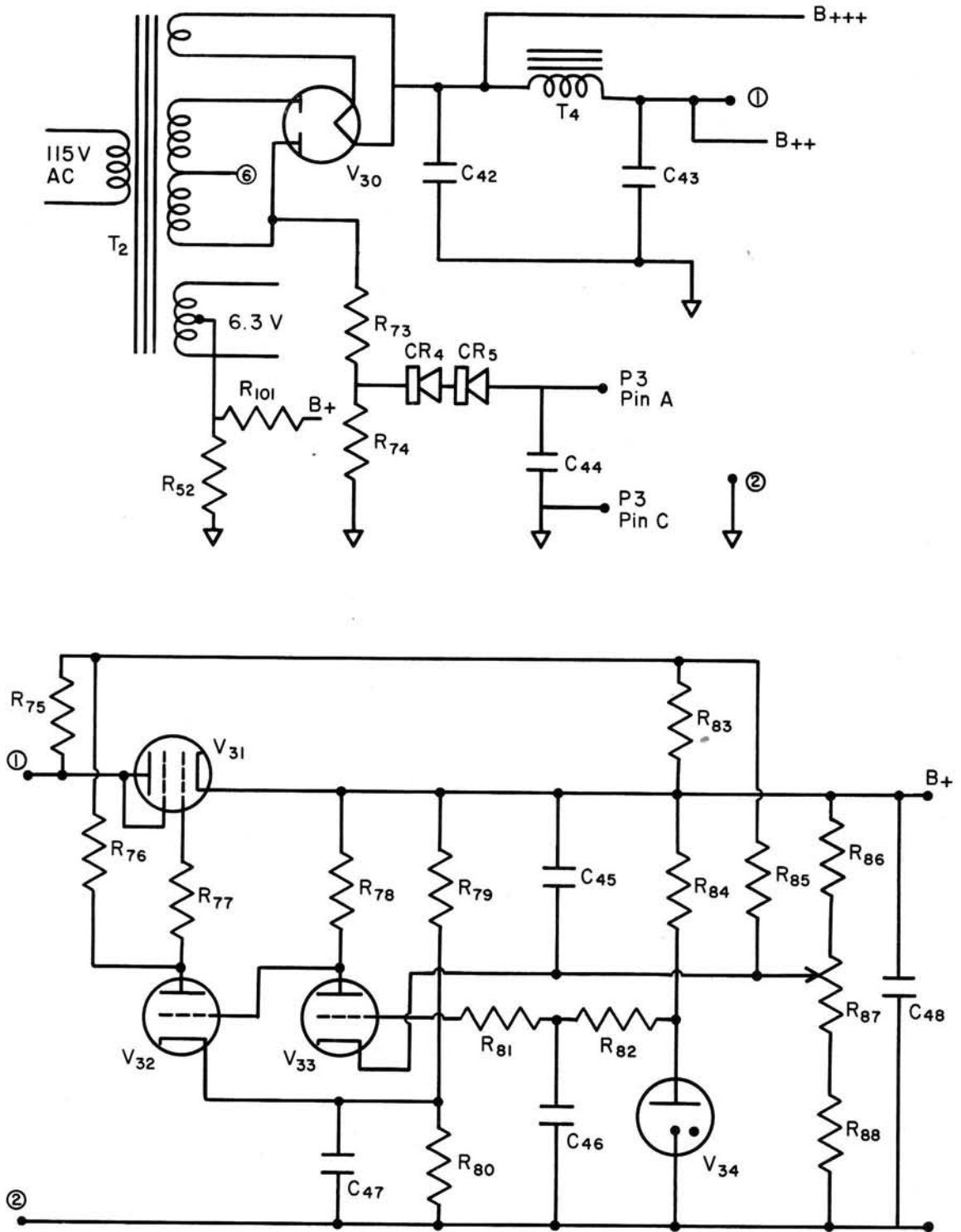


Fig. 15 - Power Supplies

P A R T S L I S T

Reference symbol code:

- (a) Fig. 11 pulser
 (b) Fig. 12 delay phantastron and amplitude discriminator
 (c) Fig. 13 amplifiers
 (d) Fig. 14 bootstrap sweep and holding circuits
 (e) Fig. 15 power supplies

V3	(V1)	6012				(a)
V9		6AS6				(c)
V10	(V21)	6AL5				(c)
V16	(V18)	12AV7				(d)
V17	(V20)	6AL5				(d)
V18	(V16)	12AV7				(d)
V20	(V17)	6AL5				(d)
V21	(V10)	6AL5				(d)
V22	(V26)	12AU7				(d)
V23	(V29)	12AU7				(d)
V24	(V25)	12AU7				(d)
V25	(V29)	12AU7				(d)
V26	(V22)	12AU7				(d)
V28		0C3				(d)
V29	(V23)	12AV7				(d)
V30		5V4				(e)
V31		6AQ5				(e)
V32	(V33)	12AX7				(e)
V33	(V32)	12AX7				(e)
V34		5651				(e)
V35	(V36)	12AV7				(b)
V36	(V35)	12AV7				(b)
V37	(38)	6U8 tube				(c)
V38	(37)	6U8 tube				(c)
Q1		2N247	(RCA)			(b)
Q2		2N247	(RCA)			(b)
Q3		2N247	(RCA)			(b)
C5	47 μ f	400 V				(a)
C6	.5 μ f	1000 V Bathtub Capacitor				(a)
C7	250 μ f	400 V				(a)
C8	1.0 μ f	50 V				(a)
C9	100 μ f	400 V				(d)
C10	.1 μ f	400 V				(d)
C11	1310 μ f	Adjustable Mica-Trimmer Combination		X1	Attenuator	(d)
C12	2620 μ f	" " " "		X2	Position	(d)
C13	3940 μ f	" " " "		X3	"	(d)

C14	5280 μmf	Adjustable Mica-Trimner Combination	X4	Attenuator	(d)
C15	7900 μmf	" " " "	X6	Position	(d)
C16	10550 μmf	" " " "	X8	"	(d)
C17	13100 μmf	" " " "	X10	"	(d)
C18	.1 μf	400 V			(a)
C19	20 μf	450 V Elect			(d)
C23	.0025 μf	400 V			(d)
C24	.005 μf	400 V			(d)
C25	.005 μf	400 V			(d)
C26	20 μf	450 V Elect			(d)
C27	20 μf	450 V Elect			(d)
C28	.05 μf	400 V			(d)
C30	.1 μf	400 V			(d)
C31	.004 μf	400 V Mica			(c)
C36	470 μmf				(b)
C37	.01 μf				(b)
C38	.002 μf	400 V			(b)
C39	.002 μf	400 V			(b)
C40	390 μmf	400 V			(b)
C41	.1 Uf	50 V Ceramic, Sprague miniaturized type P10			(b)
C42	40 μf	450 V Elect			(e)
C43	40 μf	450 V Elect			(e)
C44	20 μf	450 V Elect			(e)
C45	1 μf	600 V			(e)
C46	.1 μf	600 V			(e)
C47	4700 μmf	400 V			(e)
C48	20 μf	450 V Elect			(e)
C49	.001 μf	400 V			(d)
C51	.1 μf	50 V Ceramic, Sprague miniaturized type P10			(b)
C52	.1 μfD	400 V			(b)
C53	47 μmf	400 V			(b)
C55	680 μmf	400 V			(b)
C56	.1 μf	400 V			(b)
C57	47 μmf	400 V Ceramic Capacitor			(b)
C59	.03 μfD	400 V Paper Capacitor			(b)
C60	.05 μfD	200 V Paper Capacitor			(c)
C61	.01 μfD	600 V Ceramic Capacitor			(c)
C62	500 μfD	600 V Ceramic Capacitor			(c)
C63	1500 μfD	600 V Ceramic Capacitor			(c)
R8	100 K	$\frac{1}{2}$ watt	20%		(a)
R10	1 ohm	2 watt	20%		(a)
R11	10 K	25 watt wirewound			(a)
R14	1 meg	$\frac{1}{4}$ watt	20%		(d)
R15	820 K	$\frac{1}{2}$ watt	20%		(d)
R16	1 meg	potentiometer, <u>fine range</u>	20%		(d)
R17	10 K	1 watt	20%		(d)
R18	100 K	$\frac{1}{2}$ watt	20%		(d)
R19	100 K	1 watt	20%		(d)
R20	220 K	1 watt	20%		(d)
R21	6 K	1 watt	20%		(d)

R22	25 K	10 watt	wirewound		(d)
R24	39 K	1 watt		20%	(c)
R25	10 K	1 watt		20%	(d)
R26	39 K	1 watt		20%	(d)
R27	150 K	1 watt		20%	(d)
R28	1.8 meg	1 watt		20%	(d)
R30	2.2 meg	1 watt		20%	(d)
R32	2.2 meg	1 watt		20%	(d)
R33	10 K	1 watt		5%	(c)
R34	180 K	1 watt		5%	(c)
R35	33 K	1 watt		5%	(c)
R36	2.2 K	1 watt		5%	(c)
R37	4.7 K	1 watt		5%	(c)
R38	22 K	1 watt		5%	(c)
R39	33 K	1 watt		5%	(e)
R40	330 K	1 watt		20%	(c)
R41	1 meg	potentiometer			(c)
R45	2500 ohms	10 watt	wirewound		(d)
R46	27 ohms	1 watt		20%	(a)
R51	100 K	1 watt		20%	(d)
R52	47 K	1 watt		20%	(e)
R53	50 K	2 watt	wirewound pot		(d)
R54	33 K	1 watt		5%	(b)
R55	33 K	1 watt		5%	(b)
R56	39 K	1 watt		20%	(b)
R61	470 K	1 watt		5%	(b)
R62	680 ohms	1 watt		5%	(b)
R63	100 K	1 watt		5%	(b)
R64	470 K	1 watt		5%	(b)
R65	680 ohms	1 watt		5%	(b)
R71	100 K	potentiometer, <u>sensitivity control</u>			(b)
R72	100 K	1 watt		20%	(d)
R73	10 K	10 watt	wirewound		(e)
R74	20 K	10 watt	wirewound		(e)
R75	47 K	1 watt		20%	(e)
R76	470 K	1 watt		20%	(e)
R77	470 ohms	1 watt		20%	(e)
R78	270 K	1 watt		20%	(e)
R79	22 K	1 watt		20%	(e)
R80	47 K	1 watt		20%	(e)
R81	47 ohms	1 watt		20%	(e)
R82	47 K	1 watt		20%	(e)
R83	100 K	1 watt		20%	(e)
R84	47 K	1 watt		20%	(e)
R85	4.7 meg	1 watt		20%	(e)
R86	50 K	2 watt	wirewound		(e)
R87	10 K	2 watt	wirewound potentiometer		(e)
R88	30 K	2 watt	wirewound		(e)
R89	47 K	1 watt		20%	(d)
R90	4.7 meg	1 watt		20%	(b)
R91	680 K	1 watt		20%	(b)
R92	150 K	1 watt		20%	(b)
R93	27 K	1 watt		20%	(b)

R94	680 K	$\frac{1}{2}$ watt	20%	(b)
R95	22 K	$\frac{1}{2}$ watt	20%	(b)
R96	22 K	$\frac{1}{2}$ watt	20%	(b)
R97	470 K	$\frac{1}{2}$ watt	20%	(b)
R98	10 K	$\frac{1}{2}$ watt	20%	(b)
R99	100 K	$\frac{1}{2}$ watt	20%	(b)
R100	470 ohms	$\frac{1}{2}$ watt	20%	(b)
R101	47 K	$\frac{1}{2}$ watt	20%	(e)
R102	470 K	$\frac{1}{2}$ watt	20%	(d)
R103	100 K ohms	$\frac{1}{2}$ watt	carbon resistor	(a)
R104	10 K ohms	1 watt	$\pm 20\%$ carbon resistor	(b)
R105	10 K ohms	1 watt	$\pm 20\%$ carbon resistor	(b)
R106	100 K ohms	$\frac{1}{2}$ watt	$\pm 20\%$ carbon resistor	(b)
R107	4.7 megohm	$\frac{1}{2}$ watt	$\pm 20\%$ carbon resistor	(b)
R108	1800 ohms	1 watt	$\pm 5\%$ carbon resistor	(b)
R109	270 K ohms	$\frac{1}{2}$ watt	carbon resistor	(c)
R110	10 K ohms	$\frac{1}{2}$ watt	carbon resistor	(c)
R111	22 K ohms	1 watt	carbon resistor	(c)
R112	2700 ohms	$\frac{1}{2}$ watt	carbon resistor	(c)
R113	330 K ohms	$\frac{1}{2}$ watt	carbon resistor	(c)
R114	270 K ohms	$\frac{1}{2}$ watt	carbon resistor	(c)
R115	47 K ohms	1 watt	carbon resistor	(c)
R116	470 ohms	$\frac{1}{2}$ watt	carbon resistor	(c)
R117	1 megohm	$\frac{1}{2}$ watt	carbon resistor	(c)

The following components are contained in plug-in units manufactured by Engineering Electronics Corporation, Pasadena, California:

1st phantastron delay, Z8771:

R33, R34, R35, R36, R37, R38, V9

T1	Power transformer; primary 117 volts 60 cycles AC; secondaries: 250 V.C.T. at 25 ma, 6.3 volts at 1 ampere; Stancor PS8416	(d)
T2	Power transformer; primary 117 volts 60 cycles AC; secondaries: 750 V.C.T. at 150 ma, 5 volts at 3 amperes, 6.3 V.C.T. at 4.5 amperes; Stancor PC8411	(e)
T3	Filter choke, 16 hy, 50 ma; Stancor C1003	(d)
T4	Filter choke, 7 hy, 150 ma; Stancor C1710	(e)
T5	Filament transformer; primary 117 volts 60 cycles AC; secondary 6 volts C.T. at 3 amperes; Merit P-2946	(a)
T7	Automotive ignition coil, Mallory Voltmaster	(a)

T8	Pulse transformer; Stancor A3332	(e)
S1	SPST <u>power switch</u> , Cutler-Hammer 8280-K16	(e)
S2	60 second time delay relay, Amperite 6N060	(e)
S3	2-pole 7-position <u>coarse range</u> switch; shaft and index assembly Centralab type 300; 2 switch sections Centralab type PA-1	(d)
S4	<u>Operate-standby</u> switch, SPST, Cutler-Hammer 8280-K16	(a)
P1	<u>Power</u> connector; socket AN-3102A-16S-5P; plug AN-3106A-16S-5S	
P2	<u>Test</u> connector; socket AN-3102A-14S-2S; plug AN-3106A-14S-2P	
P3	<u>Preamplifier</u> connector; socket AN-3102A-14S7s; plug AN-3106A-14S-7P	
P4	<u>Spark coil</u> connector; socket AN-3102A-14S-9S; plug AN3106A-14S-9P	
P5	<u>Output</u> connector; socket AN-3102A-12S-3S; plug AN-3106A-12S-3P	
F1	3 ampere 250 volt fuse and Buss type HKP fuseholder	
DS1	Pilot lamp assembly, Dialco type 931 series 952208, with NE-51 neon lamp	
CR1	Sarkes-Tarzian M500 silicon rectifier and mounting clip	
CR2	" " " " " " " "	
CR3	" " " " " " " "	
CR4	" " " " " " " "	
CR5	" " " " " " " "	
CR7	IN34A	(c)
6 7	Octal tube sockets, Amphenol type 77MLP8	
3 6	7 pin miniature tube sockets with shields, Amphenol 147-913	
1	7 pin miniature tube socket, Amphenol type 147-500	
1 8	9 pin miniature tube sockets with shield, Amphenol type 59-407	
3	knobs, Johnson catalog no. 116-261	
1	chassis, aluminum, 2 in. x 17 in. x 13 in., ICA type 29023	
1	pair chassis mounting brackets, 6-1/2 in. x 10 in., Bud MB448	
1	panel, 19 in. x 8-3/4 in. x 1/8 in., Bud PA-1105-HG	
1	cabinet, steel, 19 in. x 8-3/4 in. panel space, Bud CR1551	

Bud type AC-420

ERRATA

The following corrections in Technical Paper No. 23-B should be noted:

Page 2

The first two lines of explanatory material following Eq. (1) should read:

r = measured distance (H/2 minus wave amplitude plus 5-1/2 in.)

H = wave height

Page 17

The lower graph should be labeled "Sonic." The title for this figure should read:

Fig. 7 - Comparison of Capacitive Wave Record with Sonic Wave Record, H = 1 ft, Steepness = 0.125

Page 27

<u>Change</u>	V9	6AS6	(c)	to	V9	6AS6	(b)
	V10 (V21)	6AL5	(c)		V10 (V21)	6AL5	(b)
	V16 (V18)	12AV7	(d)		V16 (V18)	12AU7	(d)
	V18 (V16)	12AV7	(d)		V18 (V16)	12AU7	(d)
	V25 (V29)	12AU7	(d)		V25 (V24)	12AU7	(d)
	V29 (V23)	12AV7	(d)		V29 (V23)	12AU7	(d)
	V35 (V36)	12AV7	(b)		V35 (V36)	12AU7	(b)
	V36 (V35)	12AV7	(b)		V36 (V35)	12AU7	(b)

Page 28

Delete

C55	680 $\mu\mu\text{f}$	400 V	(b)
C56	.1 μf	400 V	(b)

Page 29

Delete

R39	33 K	1 watt	5%	(c)
R54	33 K	$\frac{1}{2}$ watt	5%	(b)
R55	33 K	$\frac{1}{2}$ watt	5%	(b)
R61	470 K	$\frac{1}{2}$ watt	5%	(b)
R64	470 K	$\frac{1}{2}$ watt	5%	(b)
R65	680 ohms	$\frac{1}{2}$ watt	5%	(b)